Dynamic susceptibility of a concentrated ferrofluid: The role of interparticle interactions

Alexander V. Lebedev,[1] Victor I. Stepanov,[1] Andrey A. Kuznetsov,[1,2]
Alexey O. Ivanov,[3] and Alexander F. Pshenichnikov[1,2,*]

[1]*Laboratory of Dynamics of Dispersed Systems, Institute of Continuous Media Mechanics UB RAS, Korolyov Street 1, 614013 Perm, Russia*
[2]*Physics of Phase Transitions Department, Perm State University, Bukireva Street 15, 614990 Perm, Russia*
[3]*Department of Theoretical and Mathematical Physics, Institute of Natural Sciences and Mathematics, Ural Federal University, Lenin Avenue 51, 620000 Ekaterinburg, Russia*

(Received 24 December 2018; revised manuscript received 7 May 2019; published 9 September 2019)

The dynamic susceptibility of concentrated ferrofluids of magnetite-kerosene type is studied experimentally to clarify the effect of interparticle interactions on the magnetization reversal dynamics and the ferrofluid relaxation time spectrum. We synthesize six ferrofluid samples, four of which have the same wide particle size distribution with a high (more than $2kT$) average energy of magnetic dipole interactions. These samples differ in particle concentration and dynamic viscosity. The two remaining samples have a lower content of large particles and a moderate energy of magnetic dipole interactions. For all samples, we measure the dynamic susceptibility in the weak probing field at frequencies up to 160 kHz and the field amplitude dependence of the susceptibility at a frequency of 27 kHz. The results show that the susceptibility dispersion at frequencies up to 10 kHz is due to the rotational diffusion of colloidal particles and aggregates. Steric and hydrodynamic interparticle interactions are the main reason for the strong concentration dependence of the viscosity and so they also strongly influence the frequency dependence of the susceptibility. The influence of van der Waals and magnetic dipole interactions on the susceptibility is manifested indirectly, through the formation of multiparticle clusters. The contribution of clusters to the low-frequency susceptibility reaches 80%. Their large sizes (about 100 nm) shift the dispersion region to frequencies of 1–100 Hz, depending on the temperature and particle concentration. Experiments at 27 kHz demonstrate the increase in the dynamic susceptibility with increasing field amplitude. This growth is unexpected since all spectral amplitudes in the Debye function expansion of the dynamic susceptibility decrease monotonically with increasing field. To clarify the situation, the auxiliary problem of the magnetodynamics of a uniaxial particle in the alternating field is solved numerically. The Fokker-Planck-Brown rotational diffusion equation is used. It is shown that an increase in the field amplitude reduces the anisotropy barrier and the Néel relaxation time of particles and increases the dynamic susceptibility by one to two orders of magnitude compared to the weak-field limit. The calculation results are in qualitative agreement with the experimental data and allow us to propose a consistent interpretation of these data. We find that the increase in dynamic susceptibility with increasing amplitude is observed when two necessary conditions are met: (i) The suspension viscosity and the field frequency are high enough to cause the blocking of the rotational degrees of freedom of particles and aggregates and (ii) particles with a large magnetic anisotropy are present in the ferrofluid.

DOI: 10.1103/PhysRevE.100.032605

I. INTRODUCTION

A. Quasiequilibrium susceptibility of ferrofluid

Ferrofluids are an example of disordered systems with distinctive magnetic dipole interparticle interactions, which can lead to a substantial (sometimes manifold) increase of the system's initial magnetic susceptibility as compared to the susceptibility of noninteracting particles [1–5]. Over the years, many different theoretical approaches have been used to describe this effect: classical Weiss [6–8] and Onsager [9] models, the mean-spherical approximation by Wertheim and Morozov [3,10–12], the high-temperature approximation by Buyevich and Ivanov [13,14], the virial expansion technique by Morozov [15], and the cluster expansion theory by Huke and Lücke [16–18].

Later on, the modified mean-field model was frequently used to describe the equilibrium magnetization of ferrofluids. It was first proposed in [19] and was theoretically justified and refined in [20–22]. The refined version, known as the second-order modified mean-field model (MMF2), states that the equilibrium susceptibility χ_0 of the ferrofluid with strong interparticle interactions can be represented as a series expansion in powers of the Langevin susceptibility χ_L, which describes the magnetic response of noninteracting dipoles

$$\chi_0 = \chi_L\left(1 + \frac{\chi_L}{3} + \frac{\chi_L^2}{144}\right), \quad \chi_L = \frac{\mu_0 m^2 n}{3kT}, \tag{1}$$

where $\mu_0 = 4\pi \times 10^{-7}$ H/m, $m = \pi M_s x^3/6$ is the particle magnetic moment, n is the particle number concentration, M_s is the saturation magnetization of the particle material (480 kA/m for magnetite), x is the diameter of the particle magnetic core, k is the Boltzmann constant, and T is the

*pshenichnikov@icmm.ru

temperature. An important advantage of MMF2 is that it allows one to take into account in the proper manner the polydispersity of particles. To do this, it is necessary to replace the squared magnetic moment m^2 in Eq. (1) with its ensemble average $\langle m^2 \rangle$. This model is in good agreement with the experimental and numerical results for the equilibrium magnetization over a wide range of temperatures and magnetic phase concentrations [22]. The only exception is ferrofluids with a very high (of the order of 10^2) initial magnetic susceptibility. For these fluids, MMF2 underestimates the susceptibility due to inadequate consideration of the steric and magnetic dipole interactions [5].

For the monodisperse ferrofluid, the Langevin susceptibility χ_L is proportional to the product of the particle volume fraction φ by the dipolar coupling constant λ, which is the ratio of the magnetic dipole interaction energy of two particles with a minimum distance between their centers to the thermal energy

$$\chi_L = 8\lambda\varphi, \quad \lambda = \frac{\mu_0 m^2}{4\pi d^3 kT}, \quad \varphi = \frac{\pi d^3 n}{6}, \tag{2}$$

where $d = x + 2\delta$ is the particle hydrodynamic diameter and δ is the total thickness of the protective shell and the nonmagnetic layer on the particle surface. From the aforesaid it follows that Eq. (1) can be considered as a special case of the double series expansion of susceptibility in powers of φ and λ, in which only the terms containing the product of these parameters are retained. Good agreement between Eq. (1) and the experimental and numerical results [5,22] means that these terms make the main contribution to the ferrofluid initial susceptibility, at least at moderate values of φ and λ. There is a simple explanation of this fact. Both the parameter λ and the Langevin susceptibility χ_L have the meaning of the ratio of the dipole-dipole interaction energy to the thermal one. The only difference is that in the former case the interaction energy is calculated at the minimum distance between the centers of particles, which is equal to their diameter, whereas in the latter case the interaction energy is calculated at the mean distance determined by the particle number concentration n. Thus, the parameter λ defines the probability of particle aggregation and the lifetime of the formed aggregates, and the Langevin susceptibility can be treated as a measure of the intensity of magnetodipole interactions averaged over the sample volume. At small values of λ the number of aggregates in the ferrofluid is inessential and they do not affect the magnetization of the system. In this case, the Langevin susceptibility appears to be the single dimensionless parameter which defines the influence of magnetic dipole interactions on the equilibrium magnetization. So the region where Eq. (1) is valid involves low and moderate values of the dipolar coupling constant. The formation of large aggregates at $\lambda > 2$ breaks the system homogeneity at the mesoscopic and macroscopic scales, and χ_L ceases to be a universal dimensionless parameter defining the influence of interparticle interactions on the equilibrium susceptibility of the system.

Real ferrofluids, as a rule, have a wide particle size distribution, which is why an unambiguous definition of the coupling constant λ is impossible. Its numerical value depends on the problem being solved and the method of ensemble averaging [5,16,18,23–25]. In contrast, the definitions of the Langevin susceptibility and the volume fraction are straightforward:

$$\chi_L = \frac{\mu_0 \langle m^2 \rangle n}{3kT}, \quad \varphi = \frac{\pi \langle d^3 \rangle n}{6}. \tag{3}$$

For this reason, it is tempting to use the relaxation $\chi_L = 8\lambda\varphi$ in Eq. (2) as the governing equation for the dipolar coupling constant λ of the polydisperse system. It is exactly this approach that will be used in our work. Hereinafter, for the sake of convenience, the analysis and interpretation of the experimental data will be performed using the quantity

$$\lambda = \frac{\chi_L}{8\varphi} \tag{4}$$

as the dipolar coupling constant, bearing in mind that the Langevin susceptibility χ_L and hydrodynamic concentration φ are determined during independent experiments. Equation (4) allows us to accurately fit experimentally obtained dependences of the initial susceptibility on temperature and concentration at $\lambda > 2$ [5].

Ferrofluids with high initial susceptibility (tens of units) are of considerable interest to researchers as the systems in which the effects of peculiar magnetic dipole interactions are most pronounced. By that we mean the field-induced first-order phase transitions, which were repeatedly observed in laboratory experiments [24–30], and the second-order phase transitions, which were observed in numerical simulations and were predicted by some analytical models [6,31–36]. In the applied problems, a high initial susceptibility (other things being equal) increases the system's response to the weak probing field. In the latter case, the question arises about the range of applied fields, within which the ferrofluid magnetization is linearly proportional to the field and the susceptibility can be considered constant. In the quasistationary regime (i.e., at $\omega\tau \ll 1$, where ω is the field frequency and τ is the magnetization relaxation time), the condition of a weak probing field is equivalent to the smallness of the Langevin parameter ξ. If an error of the order of 1% is permissible, the condition can be written as

$$\xi = \frac{\mu_0 m H_0}{kT} \leqslant 0.3, \tag{5}$$

where H_0 is the magnetic-field amplitude. For typical commercial ferrofluids of the magnetite–liquid hydrocarbon–oleic acid type, Eq. (5) is fulfilled at $H_0 = 400$–500 A/m [37].

In an alternating magnetic field of ultrasonic frequency ($\omega\tau \sim 1$), the system susceptibility is primarily determined by the magnetization relaxation time τ and its dependence on the field value and interparticle interaction effects including particle aggregation. Although recently there have been many papers dealing with the effect of interparticle interactions on the magnetization dynamics (for example, [38–40]), the problem is still far from being solved. The available information concerns the influence of magnetic dipole interactions either on the dynamics of magnetic hard particles in a liquid or on the dynamics of superparamagnetic particles frozen into a solid matrix. Thus, according to Refs. [38–40], in ferrofluids with moderate concentrations of the magnetic phase, the magnetic dipole interaction leads to an overall increase in the imaginary part of the susceptibility and shifts its peak towards lower frequencies, whereas the relaxation time of magnetization increases by a factor of 2. Taking account of the

orientation diffusion of the magnetic moment inside the particle leads to the problem of the influence of magnetic dipole interactions on the height of the potential barrier and on the coercive force H_c. According to Refs. [41,42], the influence of the dipolar interparticle interaction on the energy barrier density depends qualitatively on the single-particle anisotropy. For low anisotropy, the shift is towards higher barriers at increasing interaction strength, whereas for moderate and high anisotropy values the shift is in the opposite direction. This interaction significantly decreases the energy barrier heights for a large fraction, at very moderate volume concentrations of particles (0.05). Similar conclusions regarding the effect of magnetic dipole interactions on the coercive force were made in [43,44]. At low values of the anisotropy energy (compared to the energy of thermal motion), the interactions lead to an increase in the local energy barriers, resulting in an increase of H_c with an increase of the packing density φ. For large values of the anisotropy energy there is a decrease in the coercive force H_c with φ.

In this work we investigate experimentally the dynamics of the magnetization reversal of concentrated ferrofluids such as magnetite in kerosene systems with a high energy of magnetic dipole interactions, a wide distribution of particles, and a high cluster content. In such a system, magnetization reversal of large particles with high magnetic anisotropy energy is due to their rotation in the liquid matrix (Brownian orientation diffusion mechanism). Therefore, the steric and hydrodynamic interactions should play an important role in the low-frequency dynamics. At frequencies of tens of kilohertz and more, the Brownian diffusion mechanism is blocked and the response of the system to the external probing field is associated only with overcoming the internal potential barriers subjected to the superimposed local magnetic fields created by neighboring particles. Hence, our main concern is to gain insight into the role of hydrodynamic interactions in highly concentrated solutions and to estimate the possible effect of magnetic dipole interactions on the Néel mechanism of magnetization reversal of single-domain particles.

B. Ferrofluid in an alternating magnetic field

In the alternating magnetic field $H = H_0 \exp(i\omega t)$, the ferrofluid magnetization changes periodically with the fundamental frequency ω and also contains high-order harmonics due to nonlinearity of the magnetization curve. Time-dependent magnetization can be expanded in the Fourier series

$$M = \sum_{k=0}^{\infty} M_k \exp\{i[(2k+1)\omega t - \Phi_k]\}, \tag{6}$$

where M_k is the amplitude of the $(2k+1)$ harmonic and Φ_k is its initial phase angle. In the weak-field limit, the magnetization is directly proportional to the field, and the right-hand side of Eq. (6) contains only the first term with $\kappa = 0$. In this case, it is convenient to introduce the coefficient of proportionality between M and H in the form of the initial dynamic susceptibility

$$\hat{\chi} = \frac{M_0}{H_0}(\cos\Phi_0 - i\sin\Phi_0) = \chi' - i\chi''. \tag{7}$$

The real and imaginary parts of Eq. (7) are responsible for the in-phase and out-of-phase components of magnetization, respectively. Here χ'' characterizes the energy dissipation in the ferrofluid. For the model system with a single relaxation time τ, the frequency dependence of the dynamic susceptibility is given by the well-known Debye formulas

$$\chi' = \frac{\chi_0}{1+\omega^2\tau^2}, \quad \chi'' = \frac{\chi_0\omega\tau}{1+\omega^2\tau^2}. \tag{8}$$

In the weak-field limit, the quantity $\chi_0 = M_0/H_0$ in Eq. (8) is clearly the equilibrium susceptibility. In strong fields, this is the linear susceptibility, i.e., the ratio between the amplitude of the fundamental harmonic of M and the field amplitude. However, real ferrofluids have a wide spectrum of relaxation times due to polydispersity of single-domain particles, the formation of clusters, and the existence of two independent relaxation mechanisms (Brownian and Néel). For this reason, Eq. (8) for real ferrofluids can be transformed into the series expansion in Debye functions. In particular, the low-frequency part of the dynamic susceptibility spectrum (which we are interested in) can be described using a relatively small number ($Q = 5$–8) of the expansion terms, each of which corresponds to a separate fraction of Brownian particles (or clusters) with the fixed relaxation time τ_i [45,46],

$$\chi'(\omega) = A_0 + \sum_{i=1}^{Q} \frac{A_i}{1+\omega^2\tau_i^2}, \quad \chi''(\omega) = \sum_{i=1}^{Q} \frac{A_i\omega\tau_i}{1+\omega^2\tau_i^2}, \tag{9}$$

where the spectral amplitudes A_i denote the contribution of the ith Brownian fraction to the equilibrium susceptibility and A_0 describes the frequency-independent (up to $\omega/2\pi \sim 10^5$ Hz) contribution of the smallest particles with the Néel relaxation mechanism. The sum of all spectral amplitudes is obviously nothing more than the equilibrium initial susceptibility. If the ith fraction is represented by individual particles, its spectral amplitude can be described by Eq. (1),

$$A_i \simeq \frac{\mu_0\langle m_i^2\rangle n_i}{3kT}\left(1 + \frac{\chi_L}{3} + \frac{\chi_L^2}{144}\right), \tag{10}$$

where n_i is the particle concentration in the ith fraction. According to Eq. (10), the spectral amplitude is proportional to the second power of the magnetic moment, i.e., to the sixth power of the magnetic core diameter. This means that the main contribution to the quasiequilibrium susceptibility is made by the coarsest fractions. Equation (10) is not suitable for the description of multiparticle clusters (aggregates), and the corresponding spectral amplitudes can be obtained from the experimental dispersion curves for the dynamic susceptibility [45,46].

As it will be shown below, the existence of two independent mechanisms of the magnetization relaxation in ferrofluids is of crucial importance for the interpretation of experimental data. Let us briefly recall these mechanisms. For a uniaxial single-domain particle embedded in a solid matrix, the most energetically favorable orientations of the magnetic moment are along or against the easy axis. These two states are separated by the energy barrier KV_m, where K is the magnetic anisotropy constant and V_m is the volume of the particle magnetic core. In the weak applied field, this barrier can be

overcome due to thermal fluctuations within the particle itself, which corresponds to the Néel relaxation mechanism [47]. The characteristic (Néel) time τ_N required to overcome the barrier grows exponentially with decreasing temperature, i.e., $\tau_N \propto \exp\sigma$, where σ is the reduced barrier height (anisotropy parameter)

$$\sigma = \frac{KV_m}{kT}. \tag{11}$$

For a more accurate estimation of the Néel relaxation time, the approximation formula

$$\tau_N = \tau_0 \frac{e^\sigma - 1}{2}\left[\frac{1}{1+1/\sigma}\sqrt{\frac{\sigma}{\pi}} + 2^{-\sigma-1}\right]^{-1} \tag{12}$$

can be used [48], where $\tau_0 \sim 10^{-9}$ s is the Larmor precession damping time. If $\omega\tau_N \gg 1$, the magnetic moment is frozen into the particle and the Néel relaxation can be neglected. In this case, the magnetic response of the particle is only due to the magnetic moment fluctuations in the vicinity of the easy axis and it can decrease by several orders of magnitude compared to the low-frequency range $\omega\tau_N \ll 1$ [49]. For a particle in a liquid matrix, i.e., for ferrofluids, the situation is different since now the moment can fluctuate due to the rotation of the particle itself. The reorientation of the easy axes provides the Brownian relaxation mechanism with the characteristic time τ_B [1],

$$\tau_B = \frac{3\eta V}{kT}, \tag{13}$$

where η is the ferrofluid dynamic viscosity and V is the particle hydrodynamic volume. The magnetization dynamics in an applied field is determined by that of two relaxation mechanisms, which ensures the shortest relaxation time.

The Brownian and Néel relaxation times depend differently on the particle volume. The condition $\tau_N = \tau_B$ gives the characteristic magnetic core diameter x^* (the so-called Shliomis diameter), which corresponds to switching out the relaxation mechanism. If $x < x^*$, then the Néel relaxation mechanism prevails, and if $x > x^*$, then the Brownian mechanism is predominant. Generally speaking, x^* does not coincide with the limiting size of superparamagnetic particles: The Brownian fraction includes both magnetically hard particles and some superparamagnetic particles with $\tau_N > \tau_B$.

Cubic crystals of magnetite exhibit a very weak crystallographic anisotropy. The effective magnetic anisotropy constant of particles K is determined to a greater degree by the shape anisotropy. The latter becomes predominant at a slight nonsphericity of particles of about a few percent. For this reason, the behavior of magnetite colloidal particles in the applied field is similar to that of uniaxial crystals, which is confirmed in particular by birefringence experiments [50,51]. For magnetite ferrofluids, according to the estimates given in Ref. [52], $x^* \approx 16$–18 nm, $\tau_N = 10^{-10}$–10^{-5} s, and $\tau_B = 10^{-5}$–10^{-3} s.

II. SAMPLE PREPARATION AND DESCRIPTION

In the experimental part of this work, our attention was focused on obtaining ferrofluid samples with a large value of the dipolar coupling constant and accordingly with a high initial susceptibility (for high particle concentrations). As can be seen from Eqs. (3) and (4), the most effective way to do this is to increase the average square of the magnetic moment $\langle m^2\rangle$ by increasing the average particle diameter and/or the relative width of the particle size distribution. To date, in the literature there have been several articles in which ferrofluids with a high (of the order of 10^2) initial susceptibility were synthesized. First of all, these are standard ferrofluids of the magnetite–liquid hydrocarbon–oleic acid type. High susceptibility was obtained by separating the coarse fraction of particles [5,53–55]. Depending on the particle concentration and temperature, the initial susceptibility varied from 60 to 120 SI units and the coupling parameter λ had a value of 2–2.5. Second, these are iron nitride–based ferrofluids with record high magnetic permeabilities reaching 180 units [56,57].

In this paper, as the base fluid we used the commercial ferrofluid prepared on the basis of aviation kerosene and finely dispersed magnetite a the broad particle size distribution manufactured by the Ivanovo State Power University. The magnetite was obtained using the standard chemical condensation method [2,58]. The desired particle size distribution was obtained by varying the synthesis conditions (concentrations of iron and ammonia salt solutions, *p*H of the medium, temperature, solution feed rate, and mixing intensity) [59]. The resulting colloidal solution was diluted to a particle volume concentration of about 6% and then was processed twice in a centrifuge equipped with four nonstandard cuvettes with a volume of 20 ml each. After each centrifugation, the particle sediment was removed. As a result of centrifugation, fine and coarse fractions with different concentrations and dispersed composition of particles were obtained. In the following, the coarse fraction was used to obtain four samples with similar size distributions of particles. These samples differed from each other only in the concentration of the magnetic phase, which ranged from 1.7 vol % to 6.6 vol %. In a few experiments, we used samples 5 and 6 with a high concentration of magnetite, obtained from the base ferrofluid and the fine fraction, respectively, by the repeated peptization method.

Magnetization curves were determined by the sweep method, in which differential magnetic susceptibility $\chi(H) = dM/dH$ of the fluid is directly measured and the magnetization curve is found by numerical integration as follows [60]:

$$M(H) = \int_0^H \chi(H)dH. \tag{14}$$

A long cooled solenoid with two galvanically isolated coaxial coils was used as the source of magnetic field. The direct current was passed through one of the coils and the weak alternating current of infralow frequency 0.1 Hz was passed through the second. The frequency was sufficiently low to ignore the relaxation processes in the ferrofluid. The design of the experimental setup made it possible to measure the amplitudes of small magnetization oscillations and the field strength, the ratio of which gave the desired value of the differential susceptibility. The dependences of the differential susceptibility on the field strength for the base ferrofluid and the fine and coarse fractions are shown in Fig. 1 and the corresponding magnetization curves are shown in Fig. 2. Figure 1 illustrates the high rate and the characteristic range of the decrease in the

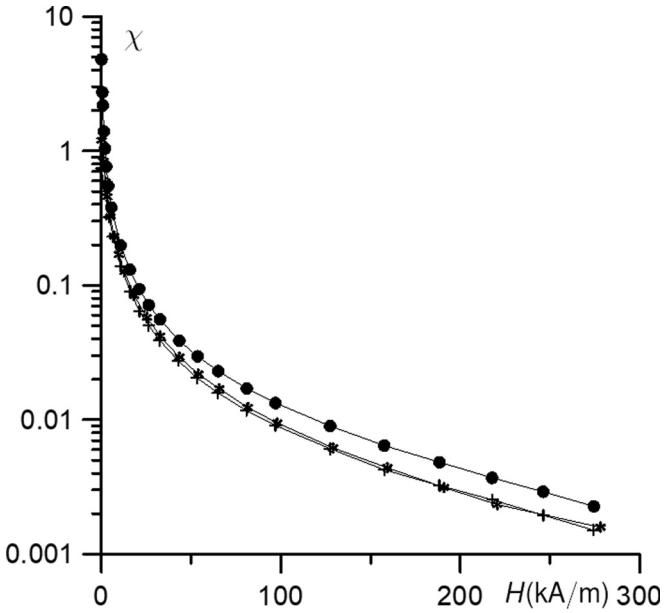

FIG. 1. Ferrofluid differential susceptibility vs the applied field: pluses, diluted base ferrofluid; asterisks, fine fraction; and circles, coarse fraction.

equilibrium susceptibility. In the probing field ranging from zero to 200 kA/m, the differential susceptibility decreases by three orders of magnitude. It can also be seen that susceptibility curves for the diluted base ferrofluid and the fine fractions are almost identical. There exists a simple explanation of what we observe in the figure. The slope of the magnetization curve in the strong fields is determined only by the temperature and

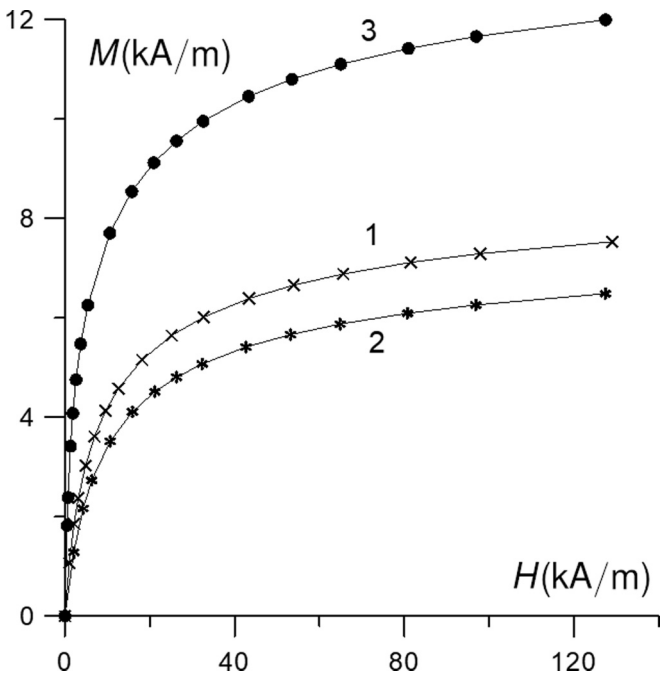

FIG. 2. Ferrofluid magnetization curves: crosses (curve 1), diluted base ferrofluid; asterisks (curve 2), fine fraction; and circles (curve 3), coarse fraction.

TABLE I. Results of the magnetogranulometric analysis.

Parameter	Commercial sample	Fine fraction	Coarse fraction
T, K	293	286	286
χ_0	4.81	0.74	4.86
M_∞ (kA/m)	27.2	7.4	13.3
n (10^{22} m^{-3})	13.6	3.85	5.79
$\langle m\rangle$ (10^{-19} A m^2)	2.00	1.92	2.31
$\langle m^2\rangle$ (10^{-37} A^2 m^2)	1.77	1.50	4.16
$\langle x\rangle$ (nm)	7.44	7.46	6.94
δ_x	0.51	0.49	0.67

the particle number concentration. The number concentrations of particles in the diluted base ferrofluid and in the fine fraction are close and so are the $\chi = \chi(H)$ curves. This means that the centrifugation of the base fluid resulted mainly in the spatial movement of the relatively small number of the largest particles from the fine fraction to the coarse one. They significantly affect the initial susceptibility (the coarse fraction susceptibility is 6.5 times larger than that of the fine fraction), but to a much lesser extent the particle concentration and the saturation magnetization (only 1.8 times larger).

The particle size distribution was determined via the magnetogranulometric analysis according to the method described in Ref. [60], which makes it possible to correctly determine the particle numerical concentration and the average magnetic moment and its average squared value. These parameters are calculated from the magnetization curve without any assumptions as to the size distribution of particles. The information on the average particle diameters and dispersions was obtained using the two-parameter Γ distribution on the assumption that the shape of the particles is not very different from that of the sphere. The Γ distribution has the form of an asymmetric bell and is described by the well-known formula

$$f(x) = \frac{x^\alpha \exp(-x/x_0)}{x_0^{\alpha+1}\Gamma(1+\alpha)}, \tag{15}$$

where $\Gamma(\alpha+1)$ is the Gamma function, x is the magnetic core diameter, x_0 and α are the distribution parameters, which are related to the average core diameter $\langle x\rangle$ and the relative distribution width δ_x by the following equations:

$$\langle x\rangle = x_0(1+\alpha), \quad \delta_x = \sqrt{\frac{\langle x^2\rangle}{\langle x\rangle^2} - 1} = \frac{1}{\sqrt{1+\alpha}}. \tag{16}$$

The basic parameters (temperature T at which the magnetization curve was measured, initial susceptibility χ_0, saturation magnetization M_∞, particle number concentration n, average magnetic moment $\langle m\rangle$, mean-square magnetic moment $\langle m^2\rangle$, and average diameter of the particle magnetic core $\langle x\rangle$) are presented in Table I for the original commercial sample and fine and coarse fractions. A comparison of the data in the table demonstrates that the average diameter of the magnetic core of the coarse fraction was even smaller than that of the original fluid. We are prone to regard this circumstance as an artifact associated with the very long tail in the particle size distribution. This tail, being formed by large particles, provides a high value of the dipolar coupling parameter, but at

TABLE II. Parameters of the samples prepared on the basis of the coarse fraction.

Sample No.	χ (at 293 K)	η (cPs) (at 293 K)	φ_m	φ_s	$\varphi(\eta)$	λ
1	2.26	1.88	0.0171	0.026	0.097	1.9
2	4.53	2.83	0.0278	0.046	0.145	2.1
3	10.5	10.3	0.0475	0.090	0.255	2.1
4	18.4	76.7	0.0659	0.146	0.332	2.2
commercial sample	4.81	20.2	0.0566	0.088	0.293	1.1

the same time introduces systematic error in the moments of high order, including $\langle x^6\rangle \sim \langle m^2\rangle$.

The parameters of samples 1–4 prepared on the basis of the coarse fraction are given in Table II. Depending on the particle concentration in the samples, their initial susceptibility varied from 2.3 to 18 (SI units), an order of magnitude less than the susceptibility of the record ferrofluids mentioned above and having approximately the same energy of magnetic dipole interactions. This result is natural since the high values of the susceptibility require low temperatures (200–240 K) and samples with saturation magnetization of about 100 kA/m [55–57]. In Table II the initial susceptibility is given for samples at room temperature whose saturation magnetization does not exceed 32 kA/m.

The volume fraction of the magnetic phase φ_m is defined as the ratio of the saturation magnetization of the sample to the saturation magnetization of the bulk magnetite, which was taken to be equal to 480 kA/m. The volume fraction of the crystalline magnetite (volume fraction of the solid phase) in the solution is calculated in terms of the ferrofluid density ρ_f under the assumption that the density of protective shells differs nonessentially from the density of kerosene $\rho_k = 0.78\ \mathrm{g/cm^3}$,

$$\varphi_s = \frac{\rho_f - \rho_k}{\rho_{\mathrm{mag}} - \rho_k},$$

where $\rho_{\mathrm{mag}} = 5.24\ \mathrm{g/cm^3}$ is the bulk magnetite density. The use of a more accurate formula allowing for φ_s is obviously due to the lack of reliable information on the effective density of the protective shell. In any case, $\varphi_s > \varphi_m$, since the spins in the surface layer of the magnetite particles do not contribute to its magnetic moment [61–64]. In general, the effective thickness δ of this nonmagnetic layer is slightly less than the crystalline lattice period and can be defined by the difference in concentrations of φ_s and φ_m. For example, for the samples presented in Table II we have $\delta = (0.74 \pm 0.05)$ nm.

The hydrodynamic particle concentration φ, which takes into account the volume of protective shells, was evaluated from the dynamic viscosity of the solutions. The dynamic viscosity η was measured with the standard Brookfield viscometer. For the Newtonian medium, such as the ferrofluid purified from an excess of stabilizer, the viscosity of the solutions is an unambiguous function of the concentration φ (see, for example, Refs. [2,65–67]). We chose the Chow approximation [65], which was tested earlier on magnetite colloids and manifested its applicability over the entire range of possible concentrations

$$\frac{\eta}{\eta_0} = \exp\left(\frac{2.5\varphi}{1-\varphi}\right) + \frac{C\varphi^2}{1 - C\gamma_m\varphi^2}, \qquad (17)$$

where η_0 is the viscosity of the carrier fluid, $C = 4.67$, and γ_m is the coefficient of dense packing of particles. Actually, the evaluation of γ_m poses a problem. Approximating the unit cell by the cubic centered lattice, Chow inferred that $\gamma_m = 0.74$, while the random dense packing of the dry particles is equal to 0.64. We instead used $\gamma_m = 0.605$, which corresponds to random packing of particles in highly concentrated suspensions, which are still capable of viscous flow [67,68]. In the strongly aggregated fluid, as is the case with the coarse fraction and samples 1–4 prepared on its basis, the multiparticle aggregates (clusters) rather than single particles should be referred to as independent kinetic units. This is the reason why the volume fraction φ of particles in the formula (17) should be replaced by the total fraction of particles and aggregates $\varphi_a = \varphi/\gamma$:

$$\frac{\eta}{\eta_0} = \exp\left(\frac{2.5\varphi}{\gamma-\varphi}\right) + \frac{C\varphi^2}{\gamma^2 - C\gamma_m\varphi^2}. \qquad (18)$$

When choosing the average packing factor of γ particles in aggregates, we were guided by the results of rheological measurements [69] in the magnetite colloids, according to which $\gamma = 0.57$.

The volume fraction of particles φ calculated by Eq. (18) and the Langevin susceptibility χ_L found from Eq. (2) were used to find the dipolar coupling constant λ [Eq. (4)], presented in Table II. As can be seen from the table, the results of the calculation of the coupling constant for samples 1–4 with identical size distributions of particles demonstrate its independence of the particle concentration, as it must be: $\lambda = 2.1 \pm 0.1$. Variations of λ do not exceed 5%, despite the fact that the concentration of the magnetic phase changes (increases) by 3.8 times, the equilibrium susceptibility of the samples changes by 8 times, the viscosity of the samples changes by 41 times, and directly measured values (equilibrium magnetic susceptibility χ and dynamic viscosity η) nonlinearly depend on the concentration of particles. The independence of the coupling constant on the particle concentration should be considered as a solid argument in favor of the selected algorithm for calculating the hydrodynamic concentration and the coupling constant.

III. DYNAMIC SUSCEPTIBILITY OF FERROFLUIDS WITH STRONG INTERPARTICLE INTERACTIONS

Much attention has been focused on the dynamics of four samples of ferrofluid mentioned above, which had similar size distributions of particles and high energy of magnetic dipole interactions, but different concentrations of the magnetic phase. The dynamic susceptibility measurements were performed using the mutual induction bridge (MIB) described previously in Ref. [37]. The schematic diagram of the MIB is

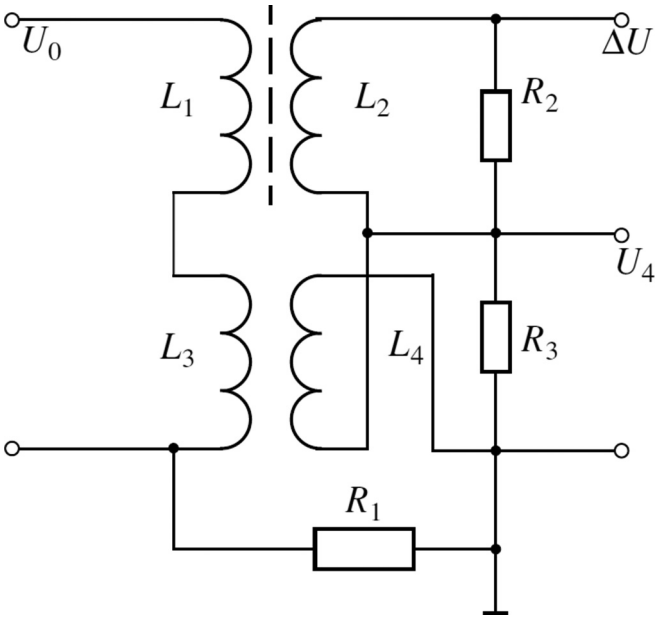

FIG. 3. Circuit diagram of the mutual-inductance bridge: L_1 and L_3 are the magnetizing solenoids, L_2 and L_4 are the measuring and compensating coils, respectively, and R_1 is the noninductive resistor.

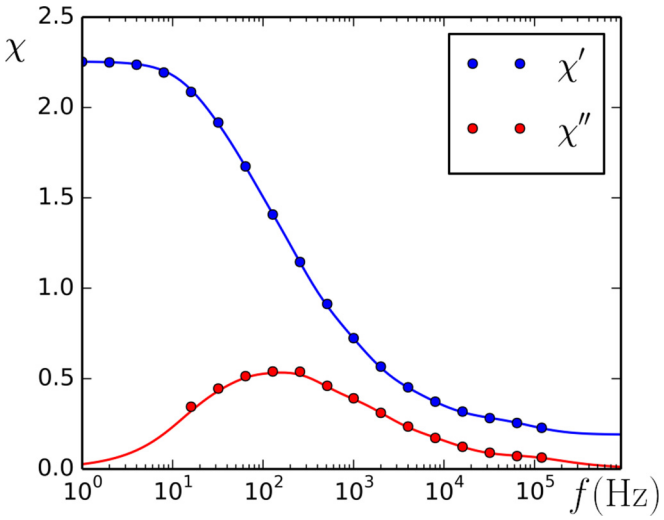

FIG. 4. Real (upper curve) and imaginary (lower curve) parts of the dynamic susceptibility of sample 1 as a function of the probing field frequency at $T = 297$ K. Circles are experimental data and solid lines are nonlinear least-squares fits of Eq. (9) with $Q = 6$.

shown in Fig. 3. Two identical spatially separated 100-mm-long and 7.8-mm-diam solenoids L_1 and L_3 had single-layer windings, which were made by winding the thin single-core copper wire around the core. The measuring coil L_2 and the identical compensating coil L_4 enclosing the middle parts of the solenoids were connected in a series-opposing fashion. The parameters of the coils were selected so that the total signal ΔU in the absence of a sample was within $2 \times 10^{-3} U_4$. The noninductive resistor R_1 served to measure the current in the magnetizing coils and determine the amplitude of the magnetic field in the sample. The high-resistance resistor R_2 served to suppress the external high-frequency interference and R_3 was used to compensate for the slight parasitic phase shift caused by resistor R_2. To reduce the parasitic capacitance, the solenoid and coil windings were applied at the compulsory winding pitch. As a result, we managed to raise the natural resonance frequency of the bridge to 2 MHz. Owing to smaller (compared to the length of the solenoids) dimensions of the measuring coils, the highly homogeneous magnetic field was generated inside them. The deviations of the field strength H inside the measuring coil from the average value were within 0.1%.

A 110-mm-long glass test tube with a cross-sectional area of 0.276 cm^2 was filled with the examined ferrofluid and placed into solenoid L_1. The fluid column was usually 105 mm in height, slightly exceeding the length of the solenoid. In the frequency range from 16 Hz to 240 kHz, the difference signal ΔU and voltage U_4 across the compensating coil L_4 were measured with the dual-channel lock-in amplifier eLockIn 203 (Anfatec), which allowed simultaneous measurements of the amplitudes and phases of two alternating voltages. At low frequencies of 0.1–8 Hz, the output signals of the bridge were measured using the 24-bit analog-to-digital converter manufactured by Rudnev–Shilyaev CJS Company. The thermostatic control of the samples was accomplished with the CRIO-VT-01 jet thermostat, which provides the working temperature range from $-30\,^\circ$C to $100\,^\circ$C.

The complex susceptibility $\hat{\chi} = \chi' - i\chi''$ related to the output voltages ΔU and U_4 by the simple equation

$$\hat{\chi} = \frac{S\Delta\hat{U}}{S_0\hat{U}_4}, \tag{19}$$

where S and S_0 are the cross-sectional areas of the coil and the sample, respectively. Equation (19) allows us to calculate the desired susceptibility components in terms of the voltages ΔU and U_4 and the phase shift between the signals. For the conditions of the experiment realized in this study (the sample in the form of the long cylinder), the demagnetizing factor of the sample was sufficiently small (0.0065 ± 0.0005) and was used for computing the correction to the difference signal ΔU. The result of the tests performed using the MIB for frequencies below 100 kHz makes it possible to determine the maximum error of the susceptibility χ' measurement, which is equal to $\pm(0.2 + 2\chi') \times 10^{-2}$. The measurement error for χ'' is at the level of 0.01 SI unit for diluted ferrofluids and does not exceed 5% of the static susceptibility value for concentrated solutions.

Figure 4 shows the frequency dependences of imaginary and real parts of the susceptibility in a weak probing field for the least concentrated sample 1 ($f = \omega/2\pi$ is the ordinary frequency). Curves demonstrate a quasi-Debye shape, which is typical for magnetite ferrofluids. The only exception here is that the region of the strongest dispersion is significantly shifted towards the low-frequency range. The size of the circles representing the experimental data in Fig. 4 corresponds to the expected measurement error, therefore the standard error bars are omitted. Solid curves in Fig. 4 correspond to the Debye function expansion (9) with seven particle fractions, including the superparamagnetic fraction with the frequency-independent susceptibility contribution (i.e., $Q = 6$). The relaxation times τ_i and the spectral amplitudes A_i in

Eq. (9) were determined from the experimental spectral curves $\chi' = \chi'(\omega)$ and $\chi'' = \chi''(\omega)$ via the method of least squares. Conditions of the minimum of the root-mean-square residual R are calculated as

$$R = \sum_j [\chi'(\omega_j) - \chi'_j]^2 + \sum_j [\chi''(\omega_j) - \chi''_j]^2 = \min,$$

where ω_j is the frequency at which the susceptibility was measured, χ'_j and χ''_j are the experimental values of its real and imaginary parts, and $\chi'(\omega_j)$ and $\chi''(\omega_j)$ are the values of its real and imaginary parts calculated from Eq. (9), respectively. To minimize the residual R, the standard Levenberg-Marquardt algorithm [70] was used.

It is apparent that the solution of the reverse problem obtained in such a way is not unique, because it depends on the selected number of fractions Q on the right-hand side of Eq. (9). With an increase of Q the error of the experimental curve approximation first decreases, reaching some irreducible level determined by the error of measurements. In all cases we chose the minimal number of fractions (from 5 to 7) capable of sustaining this irreducible level. An increase of the number of fractions above this minimum proved to be an invalid practice leading to the simultaneous increase in the error of computation of the amplitude A_i. Thus, the selection of the number of fractions Q in the series expansion (9) cannot be considered unambiguous; it involves a compromise. The desire to obtain more comprehensive information on the relaxation times and granulometric composition by increasing the number of fractions is restrained by the growth of the error in the spectral amplitude A_i; the larger the number of fractions, the greater the error. For the number of fractions chosen for our calculations the spectral amplitudes A_i are determined from Eq. (9) with an accuracy of about 20%. As for the characteristic relaxation times, they are determined up to a coefficient equal to 2. Higher accuracy is practically unattainable due to the low resolution of the method, which is based on the expansion of dispersion curves in terms of the Debye functions. Nevertheless, this accuracy is quite enough to obtain new information, since the spectrum of relaxation times of magnetite colloids is expanded by four orders of magnitude.

Since the size distribution of the particles is continuous, one might expect that instead of a discrete fit of many Debye relaxations, the continuous model will be used [71]. However, we did not use the continuous model, since in our case the main contribution to the low-frequency susceptibility is made by multiparticle clusters. As for the latter, we did not hold *a priori* information on their size distribution, which otherwise will allow us to choose a family of approximating functions.

As mentioned above, the spectral amplitude A_i is nothing but the contribution of the ith fraction of particles (or clusters) to the equilibrium susceptibility of the ferrofluid. These amplitudes and relaxation times τ_i carry information about the size of the Brownian particles. In particular, the effective hydrodynamic particle diameter can be obtained directly from Eq. (13) for the Brownian relaxation time. On the other hand, knowing the maximum size of the particle magnetic core in the colloidal solution (30–35 nm), we can estimate the corresponding maximum relaxation time. For example, for sample 1, this time is 3×10^{-5} s.

The magnetic dipole and van der Waals interparticle interactions lead to the formation of clusters, the apparent change of the characteristic sizes of particles, and the change of the contribution to static susceptibility (i.e., amplitudes A_i). This is the effect, the detection of which is one of the objectives of this study. In what follows, any group of particles with the uncompensated magnetic moment, rotating as a whole (independent kinetic unit) under the action of the weak magnetic field, will be referred to as an aggregate or cluster. The major distinguishing feature between the cluster and single particle is the cluster size. The effective diameter of the cluster must exceed the maximum possible diameter of a single particle. Clearly, clusters formed by molecular interactions and consisting of superparamagnetic particles with the Néel mechanism of relaxation only cannot be detected in this way and are eliminated from our consideration. The magnetic moments of these particles fluctuate independently of each other and the affiliation of the particles to clusters does not affect the dynamic susceptibility.

Spectral amplitudes A_i and relaxation times τ_i were obtained from a nonlinear least-squares fit of Eq. (9) to experimental points. These amplitudes and times carry information about the size and properties of Brownian particles. In particular, the effective hydrodynamic particle diameter can be obtained directly from Eq. (13) for the Brownian relaxation time. On the other hand, knowing the maximum size of the particle magnetic core in a colloidal solution (30–35 nm), one can estimate the corresponding maximum relaxation time. For sample 1, this time is 3×10^{-5} s.

Figure 5(a) shows the frequency dependences of the dynamic susceptibility modulus (normalized by its equilibrium value) for the least concentrated sample 1 and the most concentrated sample 4. The curves corresponding to samples 2 and 3 occupy intermediate positions and are not shown in the figure. The most important result, derived from Fig. 5(a), is that curves 1 and 4 can be obtained from one another by the simple shift along the frequency axis. Moreover, the whole family of dispersion curves related to samples 1–4 with similar particle size distributions can be reduced to one universal dependence of χ/χ_0 on κf due to frequency scaling [Fig. 5(b)]. The appearance of the scale factor κ is equivalent to a synchronous change of all relaxation times in Eq. (9).

According to Eq. (13), the only possible reason for this growth of relaxation times, which is the same for all particles and aggregates regardless of their size, is an increase in the effective viscosity of the suspension. The data of direct viscosity measurements on the Brookfield rotational viscometer confirm this supposition, at least qualitatively. From sample 1 to sample 4, the dynamic viscosity at $T = 293$ K increases from 1.88 to 77 mPa, i.e., by 41 times. Such a strong effect is caused by the exponential dependence of viscosity on the volume concentration of particles [65,66]. The scale factor κ is the fitting parameter, corresponding, by the order of magnitude, to an increase in the viscosity of the solution compared to the viscosity of sample 1 [see the caption to Fig. 5(b)]. Some problems with the interpretation of the results arise only due to the fact that the scaling factor κ varies less with the concentration of particles as compared to the dynamic viscosity and Brownian relaxation time in

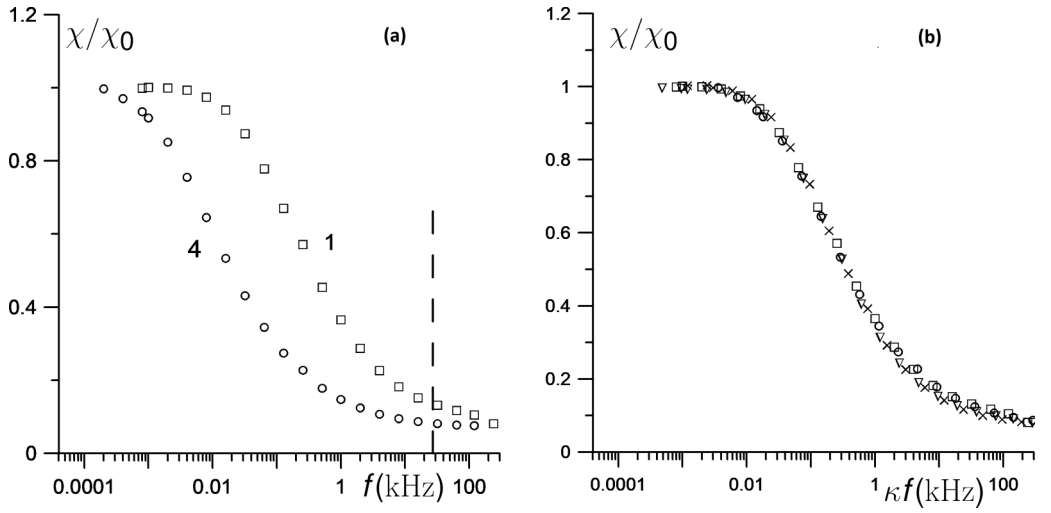

FIG. 5. Normalized modulus of the dynamic susceptibility as a function of the probing field frequency at $T = 297$ K. (a) Squares represent sample 1 and circles sample 4. The solid line is obtained by shifting curve 1 to the left along the frequency axis. The dashed vertical line shows $f = 27$ kHz. (b) The horizontal axis corresponds to the rescaled field frequency κf. Squares represent sample 1 ($\kappa = 1$), triangles sample 2 ($\kappa = 1.2$), crosses sample 3 ($\kappa = 3$) and circles sample 4 ($\kappa = 18$).

the formula (13). There are three possible reasons for this discrepancy.

(i) One is the weak effect of the Néel mechanism of magnetization reversal. If both mechanisms of rotational diffusion are in operation, then the relaxation time should be described by the more general formula as compared to Eq. (13) [1],

$$\frac{1}{\tau} = \frac{1}{\tau_B} + \frac{1}{\tau_N}, \tag{20}$$

which predicts a weaker dependence of the time of magnetization reversal on the solution viscosity.

(ii) The second is the approximate nature of Eq. (13). It was derived in the dilute solution approximation, which neglects the dependence of the particle rotational mobility on the particle concentration. The concentration dependence of the Brownian relaxation time is the direct consequence of the steric and hydrodynamic interparticle interactions. Unfortunately, there is no case of a correct description of this dependence. Here we used the heuristic approach, which is based on the assumption that the particle rotational mobility is inversely proportional to the effective suspension viscosity. Within this approach, the viscosity of the dispersion medium in Eq. (13) is replaced by the effective suspension viscosity, the concentration dependence of which is well studied [2,65–67]. This approach has proved its value for low and moderately concentrated suspensions [45,46], but it may well lead to a twofold discrepancy in the case of highly concentrated ferrofluids with a volume fraction of particles of above 40—50%.

(iii) The third possible reason for the discrepancy is magnetic dipole-dipole interactions, which are known to have a significant effect on the relaxation time spectra [38–40]. However, studies in which this influence for polydisperse ferrofluids has been estimated quantitatively are lacking.

Figure 6(a) shows the relaxation time spectrum for the least concentrated ferrofluid sample 1 (it corresponds to the fitting curves in Fig. 4). The smallest superparamagnetic particles with relaxation times lower than 10^{-7} s and frequency-independent (up to 10^5 Hz) susceptibility contribution are combined into a single fraction with the spectral amplitude A_0 because of the lack of reliable information about these particles. The six remaining fractions with the Brownian relaxation mechanism include single particles with hydrodynamic diameters up to 30 nm and relaxation times of the order of 10^{-6}–10^{-5} s and multiparticle clusters with hydrodynamic diameters of 60–250 nm, which behave as independent kinetic units with relaxation times on the order of 10^{-4}–10^{-2} s. We tend to interpret the intermediate fraction, which corresponds to an effective diameter slightly exceeding 40 nm, as the set of particle dimers. It can be seen that for sample 1 multiparticle clusters play a dominant role in the formation of the low-frequency susceptibility, while the total contribution of single particles does not exceed 15% (the same is true for other samples obtained from the coarse fraction). For comparison, Fig. 6(b) shows the relaxation time spectrum for the fine fraction, which has a dipolar coupling constant $\lambda = 1.1$ instead of the $\lambda = 2.1$ typical for the coarse fraction (see Table II). It can be seen from Fig. 6(b) that the total contribution of single particles (including superparamagnetic ones) to the low-frequency susceptibility remains almost unchanged. At the same time, the contribution of clusters decreases by almost an order of magnitude, and the equilibrium susceptibility as a whole decreases by 3.5 times. Such changes are the natural result of the ferrofluid centrifugation, during which clusters containing predominantly large particles leave the fine fraction and gather in the coarse one. Large clusters with hydrodynamic diameters of more than 100 nm and relaxation times of more than 10^{-3} s are almost absent in the fine fraction.

IV. AMPLITUDE DEPENDENCE OF THE DYNAMIC SUSCEPTIBILITY

All previous results on the dynamic susceptibility were obtained in a weak probing field of about 150 A/m, so a twofold

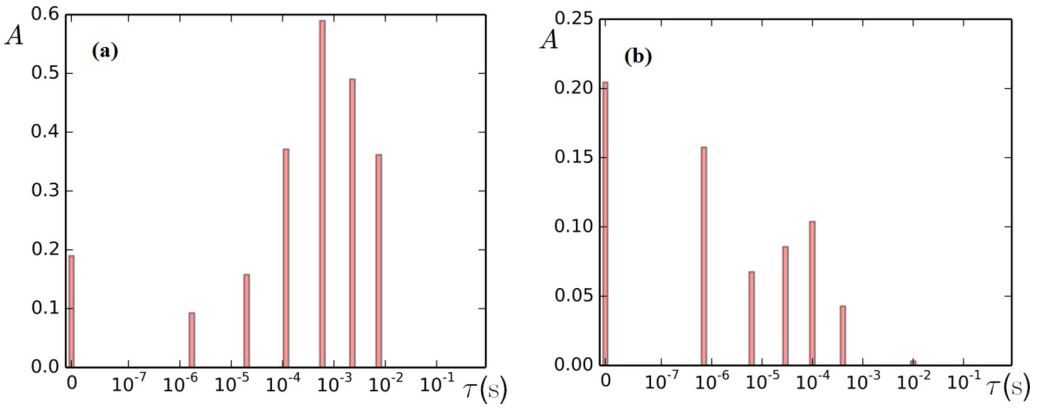

FIG. 6. Relaxation time spectrum for (a) sample 1 and (b) the fine fraction, for $T = 297$ K.

change in the field amplitude did not lead to a noticeable change in susceptibility. Dynamic measurements at increasing values of the probing field amplitude (up to 8 kA/m) were carried out with the aim of receiving a response from large aggregates and single particles, in which both relaxation mechanisms are blocked. The Brownian mechanism is blocked due to large aggregate sizes and the high suspension viscosity. The Néel mechanism is blocked due to the large magnetic anisotropy energy and correlations between the magnetic moments of neighboring particles. The tests were performed for samples 1–4, which have a strong dipolar coupling and differ only in the magnetite concentration and effective viscosity. The amplitude dependences of the dynamic susceptibility were measured at a frequency of 27 kHz, which corresponds to the vertical dashed line in Fig. 5(a). At this frequency, the dynamic susceptibility of the most concentrated sample 4 is associated only with the frequency-independent response of single superparamagnetic particles. At the same time, in the least concentrated sample 1 (whose dynamic viscosity is 41 times less), the rotational diffusion of particles still makes a marked contribution. Measurement results are shown in Fig. 7 (unlike the data presented in Fig. 5, the susceptibility modulus is not normalized and given in SI units). The sevenfold discrepancy in the dynamic susceptibility between samples 1 and 4 is due to a big difference in the magnetite concentration and approximately eightfold discrepancy in the equilibrium susceptibility.

We revealed only one but very important difference in the behavior of samples 1–4. For the least concentrated sample 1, the dynamic susceptibility modulus is almost independent of the probing field amplitude. At the same time, the susceptibility of the concentrated sample 4 increases by approximately 1.5 times as the field amplitude increases from 0 to 6 kA/m. The results for sample 1 are quite predictable, since multiparticle clusters containing large particles do not participate in the processes of magnetization reversal due to large Brownian relaxation times. As follows from Eq. (13), the main contribution to the dynamic susceptibility at 27 kHz is made by single particles with hydrodynamic diameters of about 25–30 nm and relaxation times as long as 10^{-5} s. For such particles, a magnetic field with an amplitude as large as 8 kA/m can be considered small: The Langevin parameter ξ, determined in terms of the average magnetic moment, is approximately 0.6. As for sample 4 (and to a lesser extent sample 3), an increase in susceptibility with increasing field amplitude looks very strange, since this runs contrary to Eq. (9), in which all spectral amplitudes monotonically decrease with increasing field. Indeed, for every fraction, the linear susceptibility M/H monotonically decreases with increasing H due to the fast saturation of the function $M = M(H)$. In principle, the effect can be explained by the influence of the external field on the Brownian relaxation time. It is known that the relaxation times of the longitudinal and transverse magnetization components decrease with increasing field as [1]

$$\tau_{\parallel} = \frac{\tau_B \xi L'(\xi)}{L(\xi)}, \quad \tau_{\perp} = \frac{2\tau_B L(\xi)}{\xi - L(\xi)}, \tag{21}$$

where $L(\xi) = \coth \xi - 1/\xi$ is the Langevin function. It is assumed that the sample is under the action of a constant magnetizing field, which corresponds to the Langevin parameter ξ and alternating probing field, orthogonal ($\perp$) or parallel ($\parallel$) to

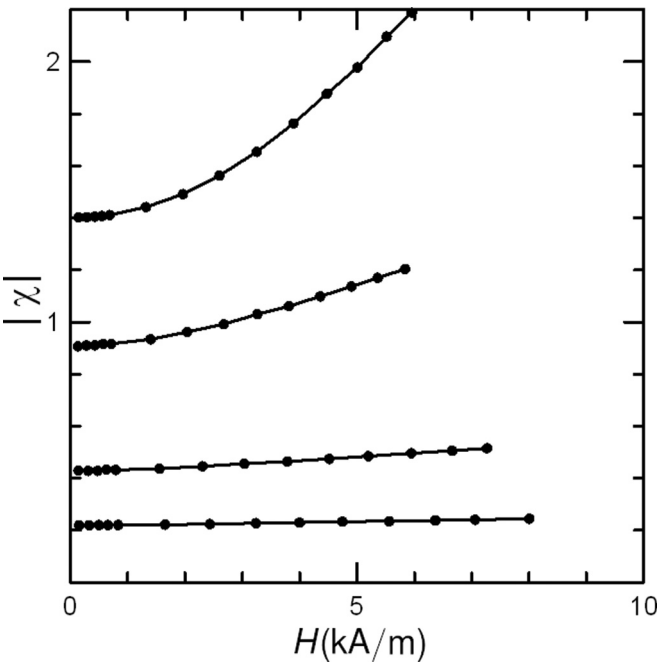

FIG. 7. Modulus of the dynamic susceptibility of four samples vs the probing field amplitude at 27 kHz. The bottom curve corresponds to sample 1 and the upper one to sample 4.

the magnetizing field. However, estimations based on Eq. (21) show that in our experiment the decrease in relaxation times does not exceed 4% and cannot explain the observed effect. Moreover, since the transition from sample 1 to sample 4 is accompanied by a 40-fold increase in the effective viscosity, one might expect the blocking of the rotational degrees of freedom of all particles and the complete deactivation of the Brownian relaxation mechanism. Only some of superparamagnetic particles with small Néel relaxation times will respond to a weak alternating field ($\omega\tau_N \leqslant 1$). If they do, then the magnetization reversal dynamics of the concentrated ferrofluid sample at tens of kilohertz should be similar to the dynamics of superparamagnetic particles embedded in the solid matrix. An example of susceptibility measurements in the solid matrix can be found in Ref. [72].

V. NUMERICAL SOLUTION OF THE PROBLEM

In order to verify the latter hypothesis, the problem of the uniaxial particle magnetodynamics in an alternating field was solved numerically. It was assumed that the particle easy axis is always parallel to the applied field. We used the Fokker-Planck-Brown rotational diffusion equation for the one-particle orientation distribution function $W(\vartheta, t)$,

$$2\tau_D \frac{\partial W}{\partial t} = \hat{\boldsymbol{J}} W \hat{\boldsymbol{J}} \left(\frac{U}{kT} + \ln W \right), \tag{22}$$

$$\frac{U}{kT} = -\sigma \cos^2 \vartheta - \xi \cos\omega t \cos\vartheta, \tag{23}$$

where ϑ is the angle between the field and the particle magnetic moment, $\tau_D = \sigma\tau_0$ is the characteristic timescale of the magnetic moment rotational diffusion, $\hat{\boldsymbol{J}} \equiv \boldsymbol{e} \times (\partial/\partial \boldsymbol{e})$ is the infinitesimal rotation operator, $\boldsymbol{e}$ is the unit vector of the magnetic moment, and U is the particle potential energy. Equation (22) was solved using the calculation technique described earlier in [49]. We calculated the statistical moments of the distribution function

$$X_l = \frac{1}{2} \int_0^\pi W(\vartheta, t) P_l(\cos\vartheta) \sin\vartheta \, d\vartheta \tag{24}$$

and their complex Fourier coefficients

$$X_{l,k}(\omega) = \frac{\omega}{2\pi} \int_0^{2\pi/\omega} X_l(t) \exp(-ik\omega t) dt. \tag{25}$$

In Eq. (24) $P_l(\cos\vartheta)$ are the Legendre polynomials. It can be readily seen that the magnetization is related to the first statistical moment as $M = nmX_1$ and the Fourier coefficients $X_{1,k}$ describe the spectral composition of the magnetization. In particular, $|X_{1,1}|/\xi$ is the analog of the linear susceptibility. The results of calculations for a probing field frequency of 27 kHz (i.e., for $\omega\tau_0 = 1.7 \times 10^{-4}$) are shown in Fig. 8 as a function of the normalized linear susceptibility modulus on the reduced field amplitude. As is evident from the figure, the amplitude dependence undergoes qualitative changes with an increasing anisotropy parameter. At $\sigma = 10$ (curve 1), the linear susceptibility monotonically decreases with increasing field amplitude, and at $\sigma = 20$ (curve 2) it monotonically increases. In the first case, the system behavior is almost quasistatic regardless of the field amplitude. However, in the second case, the amplitude plays a crucial role. For the high

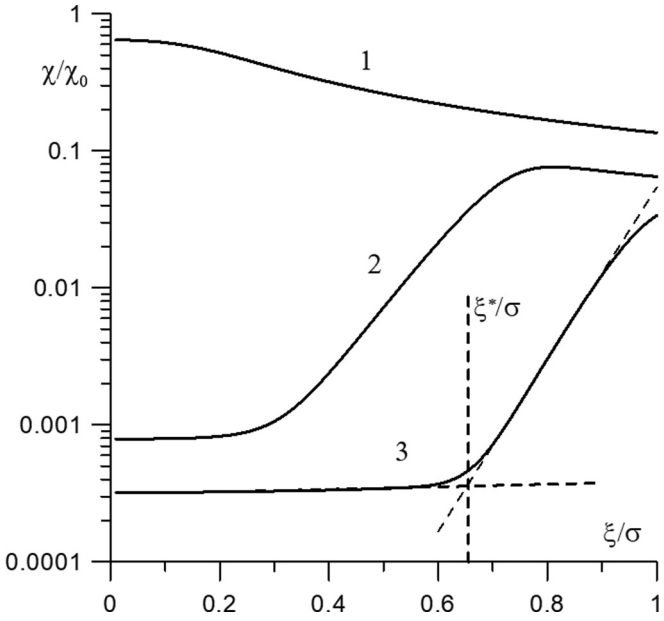

FIG. 8. Amplitude dependence of the linear susceptibility for uniaxial superparamagnetic particles at different values of the anisotropy parameter. The numerical solution of Eqs. (22) and (23) is shown at $\omega\tau_0 = 1.7 \times 10^{-4}$. Curve 1, $\sigma = 10$; curve 2, $\sigma = 20$; and curve 3, $\sigma = 30$. Dashed lines show a piecewise approximation of curve 3 and the minimum field amplitude causing the unblocking of the Néel relaxation mechanism.

anisotropy barrier, the particle response to the weak field is only due to fluctuations of the magnetic moment in the vicinity of the easy axis (since the magnetization reversal processes are blocked by the condition $\omega\tau_N \gg 1$). The linear susceptibility may decrease by several orders of magnitude compared to the equilibrium value, which is shown by curves 2 and 3 in Fig. 8. An increase in the field amplitude reduces the anisotropy barrier between the two orientations of the magnetic moment, lessens the magnetization reversal time of the system, and increases the linear susceptibility. As seen from the figure, the effect is very strong. At large field amplitudes, when the two terms on the right-hand side of Eq. (23) become comparable, the susceptibility can increase by one to two orders of magnitude compared to the limit of small amplitudes. The calculation results can be represented in a more explicit form if we approximate each curve presented in Fig. 8 with a piecewise linear function and define ξ^*/σ as the abscissa, which corresponds to the intersection of the first two segments (see dashed lines in Fig. 8). It turns out that in the whole range of parameters studied ($5 \leqslant \sigma \leqslant 30$ and $\omega\tau_0 = 1.7 \times 10^{-4}$), the results satisfy the simple formula

$$\frac{\xi^*}{\sigma} = \frac{\mu_0 M_s H^*}{K} \simeq 0.038(\sigma - \sigma^*), \quad \sigma^* \simeq 12, \tag{26}$$

where H^* is the minimum field amplitude causing the unblocking and σ^* is the minimum anisotropy parameter at which the unblocking is possible. Thus, Eq. (26) demonstrates an important feature of the dynamics of uniaxial superparamagnetic particles: The unblocking of the Néel relaxation mechanism and the concomitant increase in the dynamic susceptibility are possible only if $\sigma > \sigma^*$, i.e., if the system

contains sufficiently large particles. Under the assumption that for magnetite nanoparticles $K = (1.3–2.9) \times 10^4$ J/m^3 [52], Eq. (26) gives the following value for the minimum magnetic core diameter, for which the susceptibility can increase with increasing amplitude:

$$x_{\min} = \sqrt[3]{\frac{72kT}{\pi K}} = 17 \pm 2 \text{ nm}. \quad (27)$$

Some uncertainty in the particle diameter is due to the uncertainty in the effective magnetic anisotropy constant associated with the particle form factor and interparticle magnetic dipole interactions.

In general, Fig. 8 lends support to the view that there is a qualitative analogy between the dynamics of uniaxial superparamagnetic particles and the dynamics of the most concentrated ferrofluid sample 4 at ultrasonic frequencies. The curves plotted in the figure testify to the most probable reason for the anomalous growth of the sample susceptibility with increasing field amplitude. This is an increase in the rate of system magnetization reversal in the case when the energy of the particle-field interaction is comparable to the average height of potential barriers. The difference between the ferrofluid and the model system considered in this section is that the ferrofluid has a wide range of particle sizes and easy axis orientations. Also, the interparticle interactions effects are significant. As for the field amplitude H^*, at which the unblocking of magnetic moments is possible, it can vary from zero at $\sigma = \sigma^*$ to about 20 kA/m at $\sigma \simeq 30$ according to Eq. (26).

VI. ADDITIONAL EXPERIMENTS

In order to gain deeper insight into the roles of large particles and temperature, we conducted two additional series of experiments. In the first series, samples 5 and 6 were used, which differed from previously used samples 1–4 by a lower content of large particles. Samples 5 and 6 were obtained from the fine fraction and the base fluid, respectively (see Table I). The particle concentration in samples 5 and 6 was close to the particle concentration in sample 4, so their viscosities were also close (60–70 mPa s at room temperature). The amplitude characteristics of these samples at 27 kHz are shown in Fig. 9. From a comparison of the curves, two important conclusions can be drawn. (i) Despite the fact that the static susceptibility of sample 4 is several times greater than the susceptibility of sample 5, its dynamic susceptibility at 27 kHz is approximately half. The reason is obvious: Due to the presence of large particles and aggregates in sample 4, the effect of blocking the rotational degrees of freedom on the dynamic susceptibility is an order of magnitude stronger than that in the fine fraction. (ii) The amplitude dependence of the dynamic susceptibility of samples 5 and 6 is noticeably weaker than that of sample 4. We consider this effect as the natural result of the movement of large particles with the magnetic core diameter $x > x_{\min}$ into the coarse fraction at the centrifugation stage. This is just the result that we expected.

In the second series of experiments, we measured amplitude characteristics of sample 4 at different temperatures from 248 to 348 K. The results are shown in Fig. 10. They may seem unusual due to an increase in the dynamic susceptibility

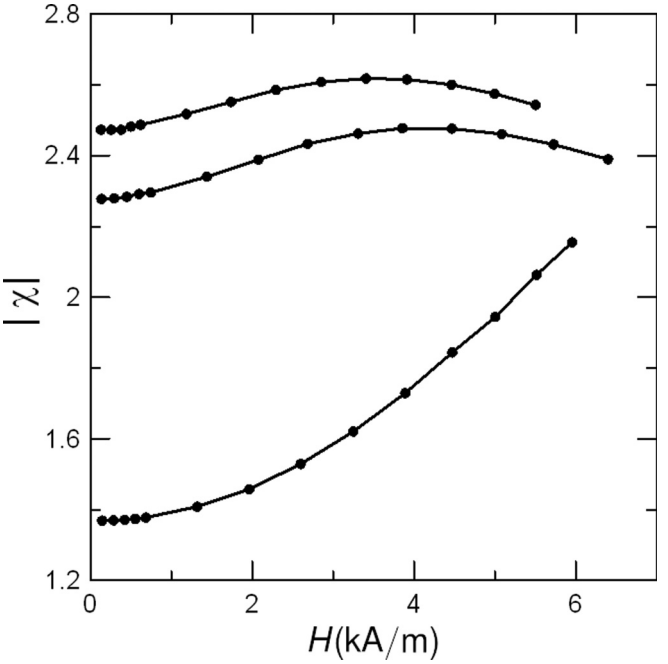

FIG. 9. Modulus of the dynamic susceptibility vs the probing field amplitude for sample 4 (bottom curve), sample 5 (upper curve), and sample 6 (middle curve) at 27 kHz.

in the weak probing field with increasing temperature. It would seem that the result should be the opposite. At least the equilibrium susceptibility defined by Eq. (1) and accordingly all spectral amplitudes in Eq. (9) always decrease with increasing temperature. However, for the dynamic susceptibility, the situation may change to the opposite due to the

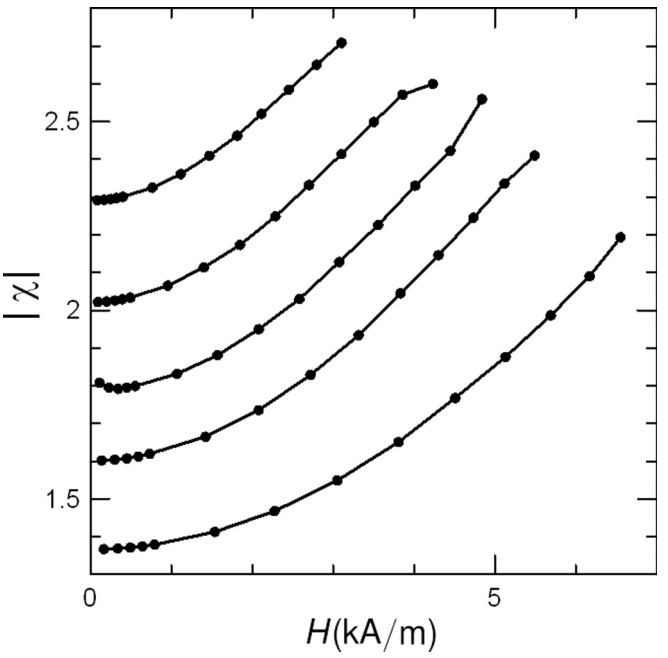

FIG. 10. Modulus of the dynamic susceptibility vs the probing field amplitude for sample 4 at different temperatures. From bottom to top, $T = 248$, 273, 298, 323, and 348 K.

temperature dependence of relaxation times [5]. This dependence is close to the exponential one: For the Néel relaxation, it follows from Eq. (12), for the Brownian relaxation, that this is due to the exponential temperature dependence of viscosity in Eq. (13) [61]. In both cases, the relaxation times in the denominators on the right-hand side of Eq. (9) quickly decrease with increasing temperature, so at sufficiently low temperatures this decrease begins to prevail over a decrease in the numerators (i.e., spectral amplitudes A_i). As a result, the dynamic susceptibility $\chi(\omega, T)$ increases until it reaches the maximum, the position of which is determined by the condition $\omega\tau(T) \simeq 1$ for the fraction making the greatest contribution to the dynamic susceptibility at a frequency ω [3,5].

Due to the high field frequency and high viscosity of sample 4, all temperatures in the range from 248 to 348 K can be considered sufficiently low, which implies that at these temperatures $\omega\tau_B(T) \gg 1$. Although in this temperature range the sample viscosity decreased 15 times (from 0.33 to 0.021 Pa s), it still remained high enough to exclude the rotational diffusion of large particles and aggregates. For particles with a diameter less than the average value (8 nm) $\omega\tau_B < 6$, and the contribution of such particles to the dynamic susceptibility at 27 kHz is noticeable. Thus, an increase in dynamic susceptibility with temperature in Fig. 10 is a natural result of the partial unblocking of the Brownian and Néel mechanisms for moderate and small particles. An increase in the probing field amplitude leads to the unblocking of the Néel relaxation mechanism even for large particles with a magnetic core diameter $x > x_{\min} \simeq 17$ nm and an additional increase in the dynamic susceptibility. Since the content of large particles is virtually independent of temperature, all the curves in Fig. 10 look qualitatively the same.

VII. DISCUSSION AND CONCLUSIONS

In this work the magnetization reversal dynamics of ferrofluids with a high energy of interparticle interactions was investigated experimentally. The aim of this work was to clarify the effect of interparticle interactions on the susceptibility dispersion and the spectrum of magnetization relaxation times.

We synthesized and investigated six samples of ferrofluid of the magnetite–oleic acid–kerosene type. The first four of them had identically wide size distributions of particles, which ensured the high average energy of magnetic dipole interactions (more than $2kT$). These four samples differed only in the nanoparticle concentration. The two remaining samples (5 and 6) had a lower content of large particles but a high total concentration. For these samples, the average energy of magnetic dipole interactions was less than $1.1kT$. For all samples, we measured the dynamic susceptibility $\chi(\omega)$ (real and imaginary parts) in a weak probing field of amplitude of 150 A/m at frequencies from 4 Hz to 160 kHz and the amplitude dependence of the susceptibility at 27 kHz. The amplitude dependence was investigated with the aim of determining the response of large aggregates and single particles without regard for the blocking of both mechanisms of the magnetic moment relaxation. The Brownian mechanism was blocked due to large aggregate sizes and a high suspension viscosity. The Néel mechanism was blocked due to a large magnetic anisotropy and correlations between neighboring particles.

The following are our main results and conclusions.

(i) Dispersion curves of the normalized dynamic susceptibility for samples with identical particle size distributions can be derived from one another by fitting the viscosity in Eq. (13) for the Brownian relaxation time. The viscosity renormalization is a sufficient procedure for describing the effect of nanoparticle concentration on the low-frequency part of the spectrum. In this frequency range, the susceptibility dispersion is due to the rotational diffusion of colloidal particles and the Brownian relaxation mechanism. Since the concentration dependences of viscosity and the Brownian relaxation time are direct consequences of the steric and hydrodynamic interparticle interactions, these interactions should be among the main factors influencing the low-frequency susceptibility. The strong effect of the van der Waals and magnetic dipole interactions on the low-frequency susceptibility manifests itself indirectly, through the formation of clusters. The contribution of clusters to the low-frequency susceptibility exceeds 80%. Their sizes (about 100 nm) shift the dispersion range towards 1–100 Hz, depending on the temperature and particle concentration.

(ii) According to Ref. [2], for typical ferrofluids that are stabilized via oleic acid, the height of the energy barrier associated with steric repulsion is close to $20kT$. This barrier ensures a negligible rate of irreversible particle aggregation and a high stability of the ferrofluid for many years. At the same time, the experiments devoted to studying the rheology and diffusion of particles in ferrofluids [69] and dynamic magnetic susceptibility [45,46] indicated a high probability of quasispherical aggregates occurring with a characteristic size of up to 100 nm, provided large particles are present. Our results have confirmed this conclusion. We suggest that defects in protective shells play an important role in the formation of nanoscale clusters in a ferrofluid stabilized by surfactant (fatty acids). The shape of the single-domain particle cannot be ideally spherical and the density of the surface coverage of the particle by surfactant molecules cannot be uniform. A local decrease in the coverage density means a decrease in the energy barrier and the occurrence of a defect.

(iii) Experiments demonstrated an increase in the dynamic susceptibility with an increase of the probing field amplitude. This increase was unexpected, since all spectral amplitudes in the expansion of the dynamic susceptibility (9) in terms of the Debye functions monotonically decrease with the field amplitude. The effect could be explained by the influence of the applied field on the Brownian relaxation time, but the estimation based on well-known dependences (21) showed that under the experimental conditions the decrease in relaxation times does not exceed 4%.

(iv) To clarify the situation with the amplitude dependence of the dynamic susceptibility, we numerically solved an auxiliary problem of the magnetodynamics of the uniaxial particle in an alternating field. We used the Fokker-Planck-Brown equation (22) for the rotational diffusion and the standard single-particle potential (23), which takes into account the magnetic anisotropy and the particle interaction with the field. The calculations elicited a picture which is qualitatively

consistent with the experimental results and gave us the key to interpret these results. An increase of the applied field amplitude leads to a decrease of the anisotropy barrier, a decrease of the system magnetization reversal rate in general, and an increase of the dynamic susceptibility. The effect is very strong: If two terms in the single-particle potential (23) becomes comparable, the susceptibility increases by one or two orders of magnitude compared to the weak-field limit.

(v) Additional important information is that the growth of the dynamic susceptibility with increasing amplitude is only possible for particles with a sufficiently high magnetic anisotropy energy KV. For the 27-kHz experiment this means the fulfillment of the condition $KV > 12kT$, which gives a minimum magnetic core diameter $x_{\min} \simeq 17$ nm. Experiments on samples 5 and 6, which have the lowest content of such particles, support this conclusion. The amplitude dependence of the susceptibility for these samples was very weak (about 5%) and not monotonic. Thus, the unusual dynamics of ferrofluid at ultrasonic frequencies, which is accompanied by an increase in the dynamic susceptibility with increasing field amplitude, is observed when the two following conditions are met. First, the suspension viscosity and the field frequency must be high enough to cause the blocking of the rotational (Brownian) degrees of freedom of free particles and aggregates. Second, the ferrofluid must contain particles with a large magnetic anisotropy ($\sigma \geqslant 12$).

(vi) We also consider it possible that the magnetic dipole interactions significantly increase the effective magnetic anisotropy constant of particles due to the inhomogeneous distribution of neighbors around the test particle and the correlation of magnetic moments, which agrees with the conclusions of Refs. [41–44]. An additional argument in favor of this assumption is the experimental results on the dynamic susceptibility of ferrofluids in the high-frequency region [52]. They demonstrated a monotonic increase in the effective magnetic anisotropy constant with increasing average magnetic dipole energy. Another similar argument is the results of numerical simulation of the magnetization reversal processes in rigid chains of superparamagnetic particles [73]. They showed that the behavior of the rigid chain in zero magnetic fields is equivalent to the behavior of a uniaxial particle with an effective anisotropy constant, which can be uniquely expressed through the dipolar coupling parameter and the number of particles in the chain.

(vii) The so-called droplike aggregates, fairly well studied experimentally and theoretically, usually consist of 10^5–10^7 particles. These macroscopic objects, up to several micrometers in size, are visible with an optical microscope and occur in both surfactant-stabilized [8,24–28] and ionic [29,74] ferrofluids due to the gas-liquid phase transition. The phase transition is observed when the bias magnetic field is an inclusion (field-induced aggregates) or the temperature is reduced or the ionic strength increases (for electrically stabilized ferrofluids). The formation of droplike aggregates disturbs the magnetic fluid uniformity at the macroscopic scale and affects the properties of the system as a whole. However, the problem of the gas-liquid phase transition induced by the external magnetic field is beyond the scope of the paper and is not considered. At low frequencies we use the weak probing field, which is not capable of initiating this transition. At high frequencies, the field amplitude reaches several kA/m, but large particles, which play a key role in the phase transition, do not respond to the field due to the large relaxation times.

(viii) All the results described here were obtained for surfactant-stabilized ferrofluids. However, we see no reason why the method of particle stabilization can qualitatively affect the dynamics of the ferrofluid in the weak probe field. For ionic ferrofluids, the particle size distribution and the effective viscosity, which is exponentially strongly dependent on particle concentration, should also remain the main parameters governing the dynamic susceptibility.

(ix) The parameters having an essential impact on the low-frequency susceptibility for surfactant-stabilized ferrofluids also include the characteristic size and concentration of nanoscale aggregates (up to 100 nm). We have no direct experimental data supporting the existence of such aggregates in ionic ferrofluids. Yet there are at least two factors indirectly indicating the probability of their appearance. (a) Particle condensation in ionic ferrofluids that manifested as a phase transition with the formation of droplike aggregates [29,74] is an indication of the important role of the attraction forces. This also means that near the phase equilibrium curve the nuclei of a new phase with a characteristic size of tens and hundreds of nanometers, i.e., nanoscale clusters, may occur. (b) In Ref. [75], by applying magnetic forces that vary strongly over the same length scale as the colloidal stabilizing force and then varying this colloidal repulsion, the authors triggered the self-assembly of the nanoparticles into parallel line patterns.

ACKNOWLEDGMENT

The research was supported by Russian Science Foundation (Grant No. 15-12-10003).

[1] M. I. Shliomis, Phys. Usp. **17**, 153 (1974).
[2] R. E. Rosensweig, *Ferrohydrodynamics* (Cambridge University Press, Cambridge, 1985).
[3] M. I. Shliomis, A. F. Pshenichnikov, K. I. Morozov, and I. Y. Shurubor, J. Magn. Magn. Mater. **85**, 40 (1990).
[4] A. F. Pshenichnikov, J. Magn. Magn. Mater. **145**, 319 (1995).
[5] A. F. Pshenichnikov and A. V. Lebedev, J. Chem. Phys. **121**, 5455 (2004).
[6] A. O. Tsebers, Magnetohydrodynamics **18**, 137 (1982).
[7] Y. I. Dikanskii, Magnetohydrodynamics **18**, 237 (1982).
[8] K. Sano and M. Doi, J. Phys. Soc. Jpn. **52**, 2810 (1983).
[9] L. Onsager, J. Am. Chem. Soc. **58**, 1486 (1936).
[10] M. S. Wertheim, J. Chem. Phys. **55**, 4291 (1971).
[11] S. A. Adelman and J. M. Deutch, J. Chem. Phys. **59**, 3971 (1973).
[12] K. I. Morozov, Bull. Acad. Sci. USSR Phys. Ser. **51**, 1073 (1987).
[13] Y. A. Buyevich and A. O. Ivanov, Physica A **190**, 276 (1992).

[14] A. O. Ivanov, Magnetohydrodynamics **28**, 353 (1992).
[15] K. I. Morozov, J. Chem. Phys. **126**, 194506 (2007).
[16] B. Huke and M. Lücke, Phys. Rev. E **62**, 6875 (2000).
[17] B. Huke and M. Lücke, J. Magn. Magn. Mater. **252**, 132 (2002).
[18] B. Huke and M. Lücke, Rep. Prog. Phys. **67**, 1731 (2004).
[19] A. F. Pshenichnikov, V. V. Mekhonoshin, and A. V. Lebedev, J. Magn. Magn. Mater. **161**, 94 (1996).
[20] A. O. Ivanov and O. B. Kuznetsova, Phys. Rev. E **64**, 041405 (2001).
[21] A. O. Ivanov and O. B. Kuznetsova, Colloid J. **68**, 430 (2006).
[22] A. O. Ivanov, S. S. Kantorovich, E. N. Reznikov, C. Holm, A. F. Pshenichnikov, A. V. Lebedev, A. Chremos, and P. J. Camp, Phys. Rev. E **75**, 061405 (2007).
[23] A. O. Ivanov and E. A. Elfimova, J. Magn. Magn. Mater. **374**, 327 (2015).
[24] A. F. Pshenichnikov and I. Y. Shurubor, Magnetohydrodynamics **24**, 417 (1988).
[25] A. S. Ivanov, J. Magn. Magn. Mater. **441**, 620 (2017).
[26] C. F. Hayes, J. Colloid Interface Sci. **52**, 239 (1975).
[27] E. A. Peterson and D. A. Krueger, J. Colloid Interface Sci. **62**, 24 (1977).
[28] A. F. Pshenichnikov and I. Y. Shurubor, Bull. Acad. Sci. USSR Phys. Ser. **51**, 1081 (1987).
[29] J.-C. Bacri, R. Perzynski, V. Cabuil, and R. Massart, J. Colloid Interface Sci. **132**, 43 (1989).
[30] A. S. Ivanov and A. F. Pshenichnikov, Phys. Fluids **26**, 012002 (2014).
[31] D. Wei and G. N. Patey, Phys. Rev. Lett. **68**, 2043 (1992).
[32] J.-J. Weis, D. Levesque, and G. J. Zarragoicoechea, Phys. Rev. Lett. **69**, 913 (1992).
[33] B. Groh and S. Dietrich, Phys. Rev. Lett. **72**, 2422 (1994).
[34] K. I. Morozov, J. Chem. Phys. **119**, 13024 (2003).
[35] A. O. Ivanov, Phys. Rev. E **68**, 011503 (2003).
[36] J.-J. Weis, J. Chem. Phys. **123**, 044503 (2005).
[37] A. F. Pshenichnikov, Instrum. Exp. Tech. **50**, 509 (2007).
[38] D. V. Berkov, L. Y. Iskakova, and A. Y. Zubarev, Phys. Rev. E **79**, 021407 (2009).
[39] A. O. Ivanov, S. S. Kantorovich, V. S. Zverev, E. A. Elfimova, A. V. Lebedev, and A. F. Pshenichnikov, Phys. Chem. Chem. Phys. **18**, 18342 (2016).
[40] A. O. Ivanov, S. S. Kantorovich, E. A. Elfimova, V. S. Zverev, J. O. Sindt, and P. J. Camp, J. Magn. Magn. Mater. **431**, 141 (2017).
[41] D. V. Berkov, N. L. Gorn, R. Schmitz, and D. Stock, J. Phys.: Condens. Matter **18**, S2595 (2006).
[42] D. V. Berkov, IEEE Trans. Magn. **38**, 2637 (2002).
[43] C. Verdes, B. Ruiz-Diaz, S. M. Thompson, R. W. Chantrell, and A. Stancu, Phys. Rev. B **65**, 174417 (2002).
[44] S. Ruta, R. Chantrell, and O. Hovorka, Sci. Rep. **5**, 9090 (2015).
[45] E. V. Lakhtina and A. F. Pshenichnikov, Colloid J. **68**, 294 (2006).
[46] A. Pshenichnikov, A. Lebedev, E. Lakhtina, and A. Kuznetsov, J. Magn. Magn. Mater. **432**, 30 (2017).
[47] L. Néel, Ann. Geophys. **5**, 99 (1949); C. R. Acad. Sci. (Paris) **228**, 664 (1949).
[48] W. T. Coffey, P. J. Cregg, D. S. F. Crothers, J. T. Waldron, and A. W. Wickstead, J. Magn. Magn. Mater. **131**, L301 (1994).
[49] Y. L. Raikher, V. I. Stepanov, and R. Perzynski, Physica B **343**, 262 (2004).
[50] Y. N. Skibin, V. V. Chekanov, and Y. L. Raikher, Zh. Eksp. Teor. Fiz. **72**, 949 (1977) [Sov. Phys. JETP **45**, 496 (1977)].
[51] V. M. Buzmakov and A. F. Pshenichnikov, Colloid J. **63**, 275 (2001).
[52] A. F. Pshenichnikov and A. V. Lebedev, Zh. Eksp. Teor. Fiz. **95**, 869 (1989) [Sov. Phys. JETP **68**, 498 (1989)].
[53] A. F. Pshenichnikov and I. Y. Shurubor, Pis'ma Zh. Tekh. Fiz. **14**, 1898 (1988) [Sov. Tech. Phys. Lett. 14, 1898 (1988)].
[54] A. F. Pshenichnikov and A. V. Lebedev, Colloid J. **57**, 800 (1995).
[55] A. F. Pshenichnikov and A. V. Lebedev, Colloid J. **67**, 189 (2005).
[56] I. Nakatani, M. Hijikata, and K. Ozawa, J. Magn. Magn. Mater. **122**, 10 (1993).
[57] H. Mamiya, I. Nakatani, and T. Furubayashi, Phys. Rev. Lett. **84**, 6106 (2000).
[58] W. C. Elmore, Phys. Rev. **54**, 309 (1938).
[59] N. M. Gribanov, E. E. Bibik, O. V. Buzunov, and V. N. Naumov, J. Magn. Magn. Mater. **85**, 7 (1990).
[60] A. F. Pshenichnikov, A. V. Lebedev, A. V. Radionov, and D. Efremov, Colloid J. **77**, 196 (2015).
[61] H. Wang, T. Zhu, K. Zhao, W. N. Wang, C. S. Wang, Y. J. Wang, and W. S. Zhan, Phys. Rev. B **70**, 092409 (2004).
[62] R. Perzynski and Y. L. Raikher, in *Surface Effects in Magnetic Nanoparticles*, edited by D. Fiorani, Nanostructure Science and Technology (Springer, New York, 2005), pp. 141–187.
[63] T. Shendruk, R. Desautels, B. Southern, and J. Van Lierop, Nanotechnology **18**, 455704 (2007).
[64] P. Dutta, S. Pal, M. Seehra, N. Shah, and G. Huffman, J. Appl. Phys. **105**, 07B501 (2009).
[65] T. S. Chow, Phys. Rev. E **50**, 1274 (1994).
[66] L. Vekas, Rom. J. Phys. **49**, 707 (2004).
[67] J. Chong, E. Christiansen, and A. Baer, J. Appl. Polym. Sci. **15**, 2007 (1971).
[68] R. Farris, Trans. Soc. Rheol. **12**, 281 (1968).
[69] V. M. Buzmakov and A. F. Pshenichnikov, J. Colloid Interface Sci. **182**, 63 (1996).
[70] D. W. Marquardt, J. Soc. Ind. Appl. Math. **11**, 431 (1963).
[71] P. C. Fannin, in *Advances in Chemical Physics*, edited by I. Prigogine and S. A. Rice (Wiley, New York, 2007), Vol. 104, pp. 181–292.
[72] S. van Berkum, J. Dee, A. Philipse, and B. Erné, Int. J. Mol. Sci. **14**, 10162 (2013).
[73] A. F. Pshenichnikov and A. A. Kuznetsov, Phys. Rev. E **92**, 042303 (2015).
[74] J.-C. Bacri, R. Perzynski, D. Salin, V. Cabuil, and R. Massart, J. Magn. Magn. Mater. **85**, 27 (1990).
[75] L. Ye, T. Pearson, Y. Cordeau, O. Mefford, and T. Crawford, Sci. Rep. **6**, 23145 (2016).